Supporting Information

Nenci et al. 10.1073/pnas.1215128109

SI Methods

Protein Expression and Purification. Unless stated otherwise, all reagents used in this work were purchased from Sigma-Aldrich. Recombinant *Cavia porcellus* alkyl-dihydroxyacetone phosphate synthase (ADPS) was expressed in *Escherichia coli* in its mature form, which lacks the N-terminal peroxisome-targeting sequence. ADPS constructs carrying either N-terminal $His_{(6)}$ or maltose-binding protein extensions yielded recombinant proteins that, although catalytically active, exhibited a strong tendency to aggregate and release flavin adenine dinucleotide (FAD). In contrast, expression of the protein in fusion with small ubiquitin-like modifier (SUMO) protein led to a dramatic improvement in holoenzyme stability, and the protein produced crystals within a few hours after proteolytic cleavage of the SUMO tag. Fusion to SUMO apparently favors proper folding of the whole protein. cDNA encoding for the mature form of ADPS (residues 76–658) was cloned into a pET SUMO vector (Invitrogen). Enzyme variants were generated using the QuikChange Site-Directed Mutagenesis Kit (Stratagene). Mutant and WT enzymes were purified using the same protocols. Plasmids were introduced into BL21-CodonPlus(DE3)-RP cells, which were grown at 37 °C in LB medium containing 50 mg/L of chloramphenicol and 50 mg/L of kanamycin. When the optical density (OD_{600}) reached a value of 0.8, 0.5 mM isopropyl-β-D-1-thiogalactopyranoside (final concentration) was added to induce overnight protein expression at 17 °C.

Cells were resuspended at 4 °C in 300 mM NaCl, 5% (vol/vol) 5 mM β-mercaptoethanol, and 50 mM Tris·HCl (pH 8.0) (buffer A). After cell disruption with a high-pressure homogenizer, crude extracts were centrifuged at 70,000 × *g*. Proteins were loaded onto a nickel-affinity His-trap column (GE Healthcare) preequilibrated in buffer A. Enzymes were eluted with 300 mM imidazole in buffer A at 4 °C and subsequently dialyzed in 50 mM NaCl, 5% (vol/vol) glycerol, and 50 mM Tris·HCl (pH 8.0) (buffer B), along with 10 μg/mL of $His_{(6)}$-tagged SUMO-protease and 100 μM FAD (final). The addition of FAD was necessary to obtain the holoenzyme, because the protein eluted from the column in the apo FAD-free form. The enzyme efficiently incorporated the cofactor, the addition of which was not necessary in the subsequent purification steps. The enzyme was loaded again a nickel-affinity column to remove the protease and the $His_{(6)}$-SUMO tag. Pooled fractions were loaded on an anion-exchange SOURCE 15Q column (GE Healthcare) equilibrated with buffer B and eluted with a linear NaCl gradient. Proteins were finally gel-filtered on a Superdex 200 10/300 GL column (GE Healthcare) preequilibrated in 50 mM NaCl, 5% (vol/vol) glycerol, and 50 mM Tris·HCl (pH 8.0).

Reconstitution with 5-deazaFAD. Reconstitution of ADPS with 5-deazaFAD was facilitated by the fact that the enzyme after the first purification step (nickel-affinity His-trap column; previous paragraph) was virtually free of bound FAD. Thus, incorporation of 5-deazaFAD was performed simply by dialysis of the partly purified apoenzyme against 5-deazariboflavin (14 μM), 1 μM FAD synthetase from *Corynebacterium ammoniagenes* (kindly provided by Dr. M. Medina, Saragoza, Spain), 10 mM $MgCl_2$, and 500 μM ATP in 50 mM NaCl, 5% (vol/vol) glycerol, and 50 mM Tris·HCl (pH 8.0). FAD synthetase generates 5-deazaFAD, which is selectively incorporated by ADPS, which does not bind riboflavin (1). The protein was then purified following the same protocol used for the FAD-bound protein. Based on inspection of the absorbance spectra, this procedure led to very good (>90%) incorporation of the cofactor analog.

Crystal Structure Analysis. Crystals were obtained by sitting-drop vapor diffusion at 20 °C by mixing equal volumes of 10 mg protein/mL in 50 mM NaCl, 5% (vol/vol) glycerol, 50 mM Tris·HCl (pH 8.0) and 30% (wt/vol) PEG1500 in 100 mM Na/Hepes (pH 7.5). Data were collected at the European Synchrotron Radiation Facility in Grenoble, France and the Swiss Light Source in Villigen, Switzerland and processed with the CCP4 package (2). The WT structure was solved by molecular replacement (3) using *Dictyostelium discoideum* ADPS as a search model. The DM (4), Coot (5), and REFMAC5 (6) programs were used for density averaging, model building, and refinement (Table S1). Mutant structures were solved starting from the WT. Figures were generated using CCP4mg (7).

Crystals of the 5-deazaFAD–reconstituted enzyme were obtained in both the presence and the absence of palmitoyl dihydroxyacetone phosphate (DHAP). The crystallization conditions were the same as used for the FAD-bound protein. Importantly, the crystals of the 5-deazaFAD ADPS grown in the presence of palmitoylDHAP were colorless, in agreement with the spectral properties of the substrate-incubated 5-deazaFAD enzyme. None of the 5-deazaFAD–containing crystals exhibited diffraction, however. The most logical explanation for this finding is that the reconstituted protein is not fully homogeneous, possibly containing a fraction of molecules in the apo state as well a fraction of protein molecules bound to FAD. This feature can be expected to inevitably cause some disorder, limiting the diffraction power. We also soaked FAD- and 5-deazaFAD–bound crystals in substrate-containing solutions, which did not cause any change in crystal color (which would be indicative of covalent adduct formation). We measured the diffraction data with FAD-bound crystals soaked in palmitoylDHAP, but the resulting electron density showed no features compatible with substrate binding, in line with the idea that the bulky substrate does not diffuse efficiently into the active site of the crystalline enzyme.

1. de Vet EC, Hilkes YH, Fraaije MW, van den Bosch H (2000) Alkyl-dihydroxyacetonephosphate synthase: Presence and role of flavin adenine dinucleotide. *J Biol Chem* 275(9):6276–6283.
2. Winn MD, et al. (2011) Overview of the CCP4 suite and current developments. *Acta Crystallogr D Biol Crystallogr* 67(Pt 4):235–242.
3. Read RJ (2001) Pushing the boundaries of molecular replacement with maximum likelihood. *Acta Crystallogr D Biol Crystallogr* 57(Pt 10):1373–1382.
4. Cowtan K, Main P (1998) Miscellaneous algorithms for density modification. *Acta Crystallogr D Biol Crystallogr* 54(Pt 4):487–493.
5. Emsley P, Lohkamp B, Scott WG, Cowtan K (2010) Features and development of Coot. *Acta Crystallogr D Biol Crystallogr* 66(Pt 4):486–501.
6. Murshudov GN, et al. (2011) REFMAC5 for the refinement of macromolecular crystal structures. *Acta Crystallogr D Biol Crystallogr* 67(Pt 4):355–367.
7. McNicholas S, Potterton E, Wilson KS, Noble ME (2011) Presenting your structures: The CCP4mg molecular-graphics software. *Acta Crystallogr D Biol Crystallogr* 67(Pt 4): 386–394.

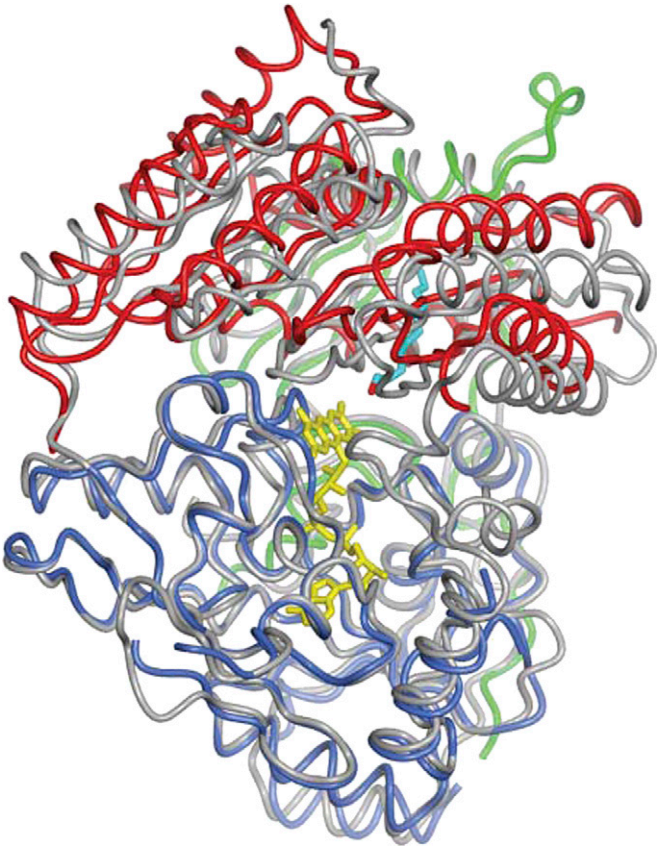

Fig. S1. Comparison of *C. porcellus* (gray; subunit C of WT structure) and *D. discoideum* ADPS structures (N-terminal domain in green, FAD domain in blue, cap domain in red; PDB ID code 2UUU). The picture was generated by superimposing the FAD domains to illustrate the 14° rotation of the cap domain, which causes a 5-Å shift in the relative positions of the two helices (α4 and α17) that shield the active site tunnel at the domain interface. The individual domains display similar tertiary structures, as indicated by the rmsd of 1.48 Å for the N-terminal domain (68 Cα atoms), 0.97 Å for the FAD-binding domain (214 Cα), and 1.33 Å for the cap domain (187 Cα). The HHH loop is ordered only in the mammalian enzyme structure.

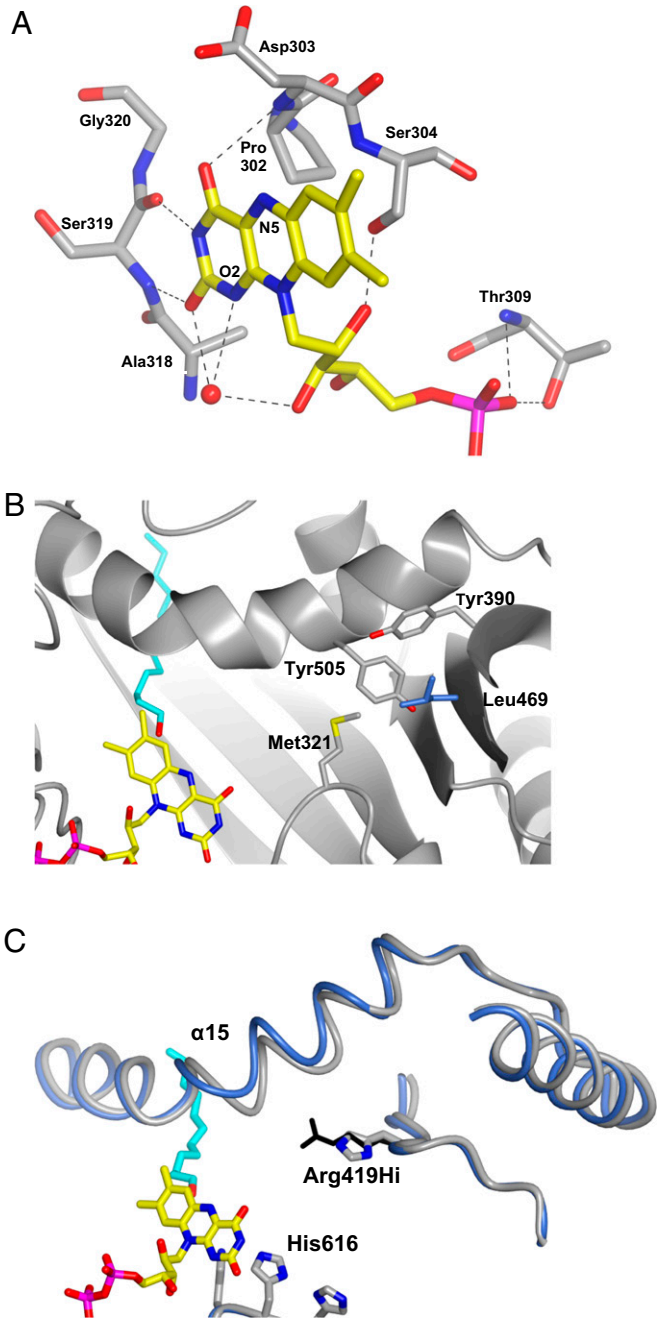

Fig. S2. Pathogenic mutations. Protein carbons are shown in gray; flavin carbons, in yellow; aliphatic ligand carbons, in cyan; oxygens, in red; nitrogens, in blue; and phosphorous, in magenta. (*A*) Thr309 directly H-bonds to the ribityl phosphate group of the FAD, and replacement with a bulky Ile residue (Thr309Ile mutant) can be expected to disrupt the site for binding the pyrophosphate moiety of the cofactor. (*B*) Leu469 is part of a hydrophobic cluster located ~12 Å from the flavin. The Leu469Pro mutant protein does not bind FAD and is difficult to purify. A plausible explanation for these findings is that despite its aliphatic nature, a Pro is not tolerated because Leu469 belongs to a β-strand with a ϕ,ψ combination (−140°, 130°), which is stereochemically unfavorable for a Pro residue. Thus, even an apparently conservative Leu-to-Pro substitution can have dramatic consequences on enzyme stability and native conformation. (*C*) Crystal structure of the Arg419His mutant. The WT protein is superimposed and shown as a blue ribbon. The WT Arg419 side chain is shown in black.

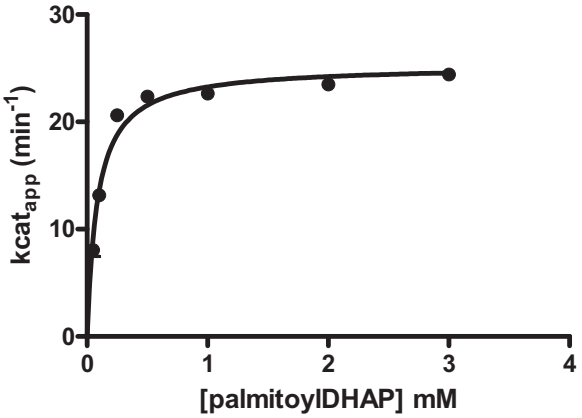

Fig. S3. Formation of DHAP from the reaction of ADPS with palmitoylDHAP. DHAP is a substrate of triose phosphate isomerase, the activity of which is monitored spectrophotometrically using an enzyme-coupled assay as described previously (1). ADPS (5 μM) was incubated with palmitoylDHAP (50–3,000 μM), 1 mM NAD^+, rabbit muscle triose phosphate isomerase (0.1 unit), 5 mM $NaAsO_2$, and rabbit muscle glyceraldehyde-3-phosphate dehydrogenase (1 unit). The reaction was performed at 25 °C in 50 mM NaCl and 50 mM Tris·HCl (pH 8.0). It was started by the addition of palmitoylDHAP. The plot shows the apparent k_{cat} values as a function of palmitoylDHAP concentrations. The measured rate constant for DHAP formation is 25.3 ± 0.51 min^{-1}. PalmitoylDHAP was prepared as a 5 mM stock solution in 50 mM Tris·HCl (pH 8.2), 50 mM NaF, and 0.1% vol/vol Triton X100.

1. O'Donoghue AC, Amyes TL, Richard JP (2005) Hydron transfer catalyzed by triosephosphate isomerase: Products of isomerization of (*R*)-glyceraldehyde 3-phosphate in D_2O. *Biochemistry* 44(7):2610–2621.

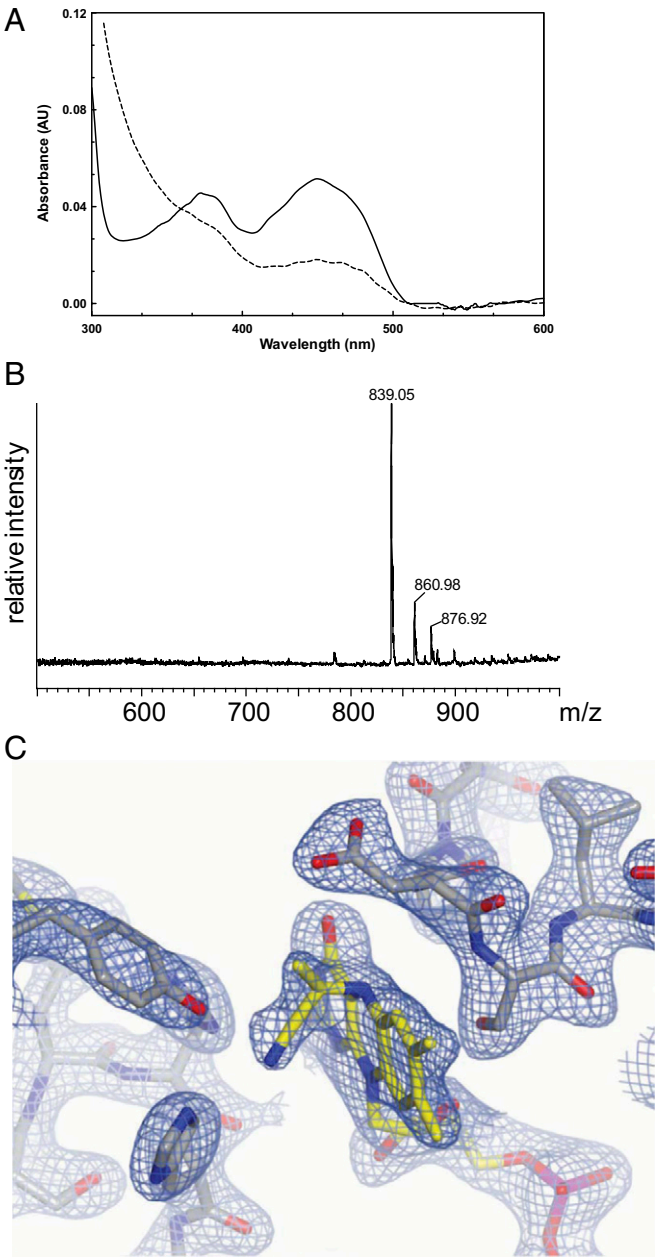

Fig. S4. Reactivity of ADPS with nitroethane. The reaction is slow (taking hours) and reversible (i.e., the enzyme gradually reoxidizes). However, as observed for nitroalkane oxidase (1), the addition of cyanide makes the process irreversible so that even on unfolding, the flavin retains a "bleached" spectrum. (*A*) ADPS [10 μM in 50 mM NaCl, 5% (vol/vol) glycerol, 50 mM Tris·HCl (pH 8.0)] was mixed with 10 mM nitroethane and 10 mM KCN (final concentrations; both previously stored as 1 M stock solutions at pH 10). After overnight incubation, the protein was unfolded by the addition of 8 M (final) urea. The spectrum was recorded after centrifugation of the denatured protein solution (dashed line). For comparison, the spectrum obtained following the same procedure but in the absence of nitroethane is also shown (solid line). The spectrum of the FAD released from the nitroethane-incubated protein is fully consistent with the presence of 5-cyanoethylFAD. (*B*) Formation of this adduct was confirmed by electrospray-ionization MS of the cofactor released after protein denaturation. ADPS was incubated with ligands as described in *A*, and buffer was exchanged into 150 mM ammonium acetate (pH 7.5). To allow release of the 5-(1-cyanoethyl)-FAD, the complex was diluted with 10% formic acid and sprayed in negative mode on a Waters LCT electrospray-TOF mass spectrometer using borosilicate capillaries created in house using a Sutter P-97 micropipette puller and an Edwards Scancoat Six sputter coater. The theoretical mass of 839.6 Da matches the observed molecular mass of 839.05 Da. (*C*) Crystal structure of 5-cyanoethylFAD ADPS. The protein was incubated overnight with nitroethane and cyanide as in Fig. S4*A*, then buffer-exchanged and concentrated to 10 mg protein/mL in 50 mM NaCl, 5% (vol/vol) glycerol, and 50 mM Tris·HCl (pH 8.0). Crystals were obtained under the same conditions used for the unbound enzyme. The picture shows the final 2Fo-Fc–weighted electron density map contoured at the 1.5-σ level and at 2.4-Å resolution (Table S1).

1. Valley MP, Tichy SE, Fitzpatrick PF (2005) Establishing the kinetic competency of the cationic imine intermediate in nitroalkane oxidase. *J Am Chem Soc* 127(7):2062–2066.

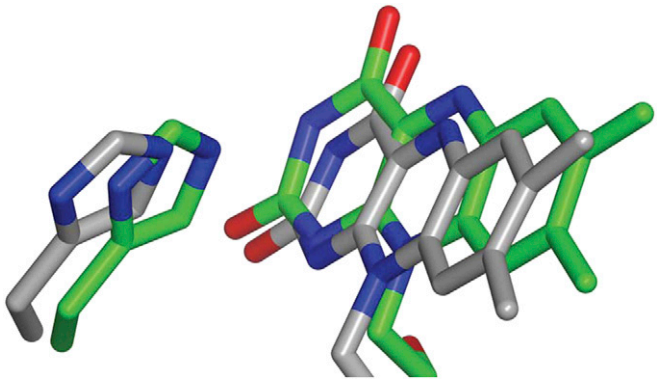

Fig. S5. Superposition of the active site of ADPS (carbons in gray) and the active site of D-lactate dehydrogenase (carbons in green; PDB ID code 1F0X), an enzyme of the same structural class as ADPS. The two enzymes share a conserved His side chain (His617 in ADPS), proposed to form an H-bond interaction with the oxygen atoms of their substrates.

Table S1. Crystallography data

	WT	R419H	Y578F	Cyanoethyl complex
PDB ID code*	4BBY	4BC7	4BCA	4BC9
Unit cell axes, Å	61.3, 99.2, 107.8	61.4, 99.2, 107.5	61.7, 99.3, 108.0	60.9, 98.6, 106.2
Unit cell angles, °	90.4, 92.2, 94.9	90.6, 91.9, 95.0	90.4, 92.1, 95.7	90.9, 89.9, 95,6
Resolution, Å	1.9	2.4	2.4	2.4
R_{merge}, %†	15.1 (36.3)	9.3 (41.9)	16.4 (74.9)	12.3 (57.8)
Completeness, %†	91.8 (78.4)	95.4 (95.3)	98.6 (98.0)	97.7 (97.0)
Unique reflections†	184,434 (23,040)	94,192 (13,781)	98,369 (14,264)	92,832 (13,475)
Multiplicity†	2.7 (1.8)	2.1 (2.1)	4.4 (4.4)	4.1 (4.1)
R_{cryst}, %	19.2	21.1	18.7	18.7
R_{free}, %	23.9	26.9	25.2	24.7
rmsd bond length, Å	0.023	0.020	0.019	0.012
rmsd bond angles, °	2.2	1.7	1.8	1.6
Ramchandran outliers	0.1%	0.1%	0.2%	0.1%

*Crystals contain four enzyme monomers in the unit cell with space group P1. Strict noncrystallographic symmetry restraints were applied through the refinements.
†Data for the highest-resolution shell are in parentheses.